DARK STARS: A NEW LOOK AT THE FIRST STARS IN THE UNIVERSE

Douglas Spolyar[1], Peter Bodenheimer[2], Katherine Freese[3], and Paolo Gondolo[4]

Draft version March 18, 2009

ABSTRACT

We have proposed that the first phase of stellar evolution in the history of the Universe may be Dark Stars (DS), powered by dark matter heating rather than by nuclear fusion, and in this paper we examine the history of these DS. The power source is annihilation of Weakly Interacting Massive Particles (WIMPs) which are their own antiparticles. These WIMPs are the best motivated dark matter (DM) candidates and may be discovered by ongoing direct or indirect detection searches (e.g. FERMI/GLAST) or at the Large Hadron Collider at CERN. A new stellar phase results, powered by DM annihilation as long as there is DM fuel, from millions to billions of years. We build up the dark stars from the time DM heating becomes the dominant power source, accreting more and more matter onto them. We have included many new effects in the current study, including a variety of particle masses and accretion rates, nuclear burning, feedback mechanisms, and possible repopulation of DM density due to capture. Remarkably, we find that in all these cases, we obtain the same result: the first stars are very large, 500-1000 times as massive as the Sun; as well as puffy (radii 1-10 A.U.), bright ($10^6 - 10^7 L_\odot$), and cool ($T_{surf} <$10,000 K) during the accretion. These results differ markedly from the standard picture in the absence of DM heating, in which the maximum mass is about 140 $M_\odot$ (McKee & Tan 2008) and the temperatures are much hotter ($T_{surf} >$50,000K). Hence DS should be observationally distinct from standard Pop III stars. In addition, DS avoid the (unobserved) element enrichment produced by the standard first stars. Once the dark matter fuel is exhausted, the DS becomes a heavy main sequence star; these stars eventually collapse to form massive black holes that may provide seeds for the supermassive black holes observed at early times as well as explanations for recent ARCADE data (Seiffert et al. 2009) and for intermediate mass black holes.

Subject headings: Dark Matter, Star Formation, Accretion

1. INTRODUCTION

Spolyar et al. (2008; hereafter Paper I) proposed a new phase of stellar evolution: the first stars to form in the Universe may be Dark Stars, powered by dark matter heating rather than by nuclear fusion. Here dark matter (DM), while constituting a negligible fraction of the star's mass, provides the energy source that powers the star. The first stars in the Universe mark the end of the cosmic dark ages, provide the enriched gas required for later stellar generations, contribute to reionization, and may be precursors to black holes that coalesce and power bright early quasars. One of the outstanding problems in astrophysics is to investigate the mass and properties of these first stars. Depending on their initial masses, the stars lead very different lives, produce very different elemental enrichment, and end up as very different objects. In this paper, we find the mass, luminosity, temperature, and radius of dark stars as a function of time: our results differ in important ways from the standard picture of first stars without DM heating.

The DM particles considered here are Weakly Interacting Massive Particles (WIMPS), such as the lightest supersymmetric particles or Kaluza-Klein dark matter

Electronic address: ktfreese@umich.edu
Electronic address: peter@ucolick.org
Electronic address: dspolyar@physics.ucsc.edu
Electronic address: paolo@physics.utah.edu
[1] Physics Dept., University of California, Santa Cruz, CA 95064
[2] UCO/Lick Observatory and Dept. of Astronomy and Astrophysics, University of California, Santa Cruz, CA 95064
[3] Michigan Center for Theoretical Physics, Physics Dept., Univ. of Michigan, Ann Arbor, MI 48109
[4] Physics Dept., University of Utah, Salt Lake City, UT 84112

(for reviews, see Jungman et al. 1996; Bertone et al. 2005; Hooper & Profumo 2007). The search for these particles is one of the major motivations for the Large Hadron Collider at CERN. The particles in consideration are their own antiparticles; thus, they annihilate among themselves in the early universe and naturally provide the correct relic density today to explain the dark matter of the universe. The first stars are particularly good sites for DM annihilation because they form in a very high density DM environment: they form at early times at high redshifts (density scales as $(1 + z)^3$) and in the high density centers of DM haloes. The first stars form at redshifts $z \sim 10 - 50$ in DM halos of $10^6 M_\odot$ (for reviews see e.g. Ripamonti & Abel 2005; Barkana & Loeb 2001; Yoshida et al. 2003; Bromm & Larson 2004; see also Yoshida et al. 2006) One star is thought to form inside one such DM halo. These halos consist of 85% DM and 15% baryons in the form of metal-free gas made of H and He. Theoretical calculations indicate that the baryonic matter cools and collapses via H_2 cooling (Peebles & Dicke 1968; Matsuda et al. 1971; Hollenbach & McKee 1979) into a single small protostar (Omukai & Nishi 1998) at the center of the halo.

As our canonical values, we use the standard $\langle \sigma v \rangle = 3 \times 10^{-26}$ cm³/s for the annihilation cross section and $m_\chi = 100$ GeV for the WIMP particle mass. In this paper we examine a variety of possible WIMP masses and cross sections, and find that our main result holds independent of these properties. We consider $m_\chi = 1$ GeV, 10 GeV, 100 GeV, 1 TeV, and 10 TeV. This variety of WIMP masses may be traded for a variety of values of the annihilation cross section, since DM heating scales

as $\langle \sigma v \rangle / m_\chi$.

Paper I found that DM annihilation provides a powerful heat source in the first stars, a source so intense that its heating overwhelms all cooling mechanisms; subsequent work has found that the heating can dominate over fusion as well once it becomes important at later stages (see below). Paper I outlined the three key ingredients for Dark Stars: 1) high dark matter densities, 2) the annihilation products get trapped inside the star, and 3) DM heating wins over other cooling or heating mechanisms. These same ingredients are required throughout the evolution of the dark stars, whether during the protostellar phase or during the main sequence phase.

WIMP annihilation produces energy at a rate per unit volume

$$\hat{Q}_{DM} = \langle \sigma v \rangle \rho_\chi^2 / m_\chi, \tag{1}$$

where ρ_χ is the mass density of the WIMPs. Once the gas density of the collapsing protostar exceeds a critical value, most of the annihilation energy is trapped in the star. For a 100 GeV particle, when the hydrogen density reaches $\sim 10^{13} \, \mathrm{cm}^{-3}$, typically 1/3 of the energy is lost to neutrinos that escape the star, while the other 2/3 of the energy is trapped inside the star. Hence the luminosity from the DM heating is

$$L_{DM} \sim \frac{2}{3} \int \hat{Q}_{DM} dV \tag{2}$$

where dV is the volume element. From this point forwards, the DM heating beats any cooling mechanisms. This point is the beginning of the life of the dark star, a DM powered star which lasts until the DM fuel runs out. The DM constitutes a negligible fraction of the mass of the dark star (less than one percent of the total stellar mass) and yet powers the star. This "power of darkness" is due to the 67% efficiency of converting the DM mass into an energy source for the star, in contrast to the $\sim 1\%$ efficiency of converting nuclear mass into energy in the case of fusion.

In this paper we ascertain the properties of the dark star as it grows from an initially small mass at its inception to its final fate as a very large star. At the beginning, when the DM heating first dominates inside the star, the dark star mass for our canonical case of 100 GeV mass particles is $0.6 M_\odot$ with a radius of 17 AU (Abel et al. 2002; Gao et al. 2007). Then further matter can rain down upon the star, causing the dark star to grow. By the time the star reaches about 3 $\mathrm{M}_\odot$, with a radius of 1–10 AU, it can be approximated as an object in thermal and hydrostatic equilibrium, with dark matter heating balancing the radiated luminosity. There is $\sim 1000 M_\odot$ of unstable gas ($\sim$ Jeans mass) which can in principle accrete onto the star, unless there is some feedback to stop it. We build up the dark star from a few solar masses by accretion, in steps of one solar mass. At each stage we find the stellar structure as a polytrope in hydrostatic and thermal equilibrium. We continue this process of building up the DS until the DM runs out.

As seen in equation (1), a key element in the annihilation is knowledge of the DM density inside the DS. The initial DM density profile in the $10^6 M_\odot$ halo is not enough to drive DM heating. We consider three mechanisms for enhancing the density. First, as originally proposed in Paper 1 and confirmed in Freese et al (2008b),

adiabatic contraction (AC) drives up the density. As the gas collapses into the star, DM is gravitationally pulled along with it. Second, as the DS accretes more baryonic matter, again DM falls in along with the gas. Eventually the supply of DM due to this continued AC runs out, and the star may heat up until fusion sets in. However, there is the possibility of repopulating the DM in the DS due to a third source of DM, capture from the ambient medium (Iocco 2008; Freese et al. 2008c). Capture only becomes important once the DS is already large (hundreds of solar masses), and only with the additional particle physics ingredient of a significant WIMP/nucleon elastic scattering cross section at or near the current experimental bounds. Capture can be important as long as the DS resides in a sufficiently high density environment. In this case the DS lives until it leaves the womb at the untouched center of a $10^6 M_\odot$ DM halo. Unfortunately for the DS, such a comfortable home is not likely to persist for more than 10-100 Myr (if the simulations are right), though in the extreme case one may hope that they survive to the present day. In this paper we consider all three mechanisms for DM enhancement, including DM capture. We remark at the outset that AC is absolutely essential to the existence of the DS. None of these three mechanisms would operate were it not for some AC driving up the density in the vicinity of the DS.

Previously (Freese et al. 2008a), we considered one specific case, that of 100 GeV particle mass and a constant accretion rate of $2 \times 10^{-3} M_\odot$/yr with no capture, assuming that the DS stellar structure can be described by a series of $n = 3/2$ polytropes. We found that it takes ~ 0.5 million years to build up the star to its final mass, which we found to be very large, $\sim 800 M_\odot$. While the accretion was in process, the dark stars were quite bright and cool, with luminosities $L \sim 10^6 L_\odot$ and surface temperatures $T_{surf} < 10,000 K$. These results are in contrast to the standard properties of the Population III stars (the first stars). Standard Pop III stars are predicted to form by accretion onto a much smaller protostar ($10^{-3} M_\odot$; Omukai & Nishi 1998), to reach much hotter surface temperatures $T_{\mathrm{surf}} \gg 50,000$ K during accretion, and at the end of accretion to be far less massive ($\sim 100 - 200 M_\odot$) due to a variety of feedback mechanisms that stop accretion of the gas (McKee and Tan 2008). These differences in properties between dark stars and standard Pop III stars lead to a universe that can look quite different, as discussed below.

In this paper we present the results of a complete study of building up the dark star mass and finding the stellar structure at each step in mass accretion. We include many new effects in this paper compared to Freese et al. (2008a). (1) We generalize the particle physics parameters by considering a variety of particle masses or equivalently annihilation cross sections. (2) We study two possible accretion rates: a variable accretion rate from Tan & McKee (2004) and an alternate variable accretion rate found by O'Shea & Norman (2007). (3) Whereas previously we considered only $n = 3/2$ polytropes, which should be used only when convection dominates, we now allow variable polytropic index to include the transition to radiative transport ($n = 3$). (4) We include gravity as a heat source. In the later stages of accretion, as the DM begins to run out and the star begins to contract, the gravitational potential energy is converted to an im-

portant power source. (5) We include nuclear burning, which becomes important once the DM starts to run out. (6) We include feedback mechanisms which can prevent further accretion. Once the stellar surface becomes hot enough, again when the DM is running out, the radiation can prevent accretion. (7) We include the effects of repopulating the DM inside the star via capture from the ambient medium. The result of this paper is that, for all the variety of parameter choices we consider, and with all the physical effects included, with and without capture, our basic result is the same. The final stellar mass is driven to be very high and, while DM reigns, the star remains bright but cool.

Other work on dark-matter contraction, capture, and annihilation in the first stars (Freese et al. 2008c; Taoso et al. 2008; Yoon et al. 2008; Iocco et al. 2008; Ripamonti et al. 2009) has concentrated on the case of the pre-main-sequence, main-sequence, and post-main-sequence evolution of stars at fixed mass, in contrast to the present work, which allows for accretion from the dark-matter halo.

We also cite previous work on DM annihilation in today's stars (less powerful than in the first stars): Krauss et al. (1985); Bouquet & Salati (1989); Salati & Silk (1989); Moskalenko & Wai (2007); Scott et al. (2007); Bertone & Fairbairn (2007); Scott et al. (2009).

2. EQUILIBRIUM STRUCTURE

2.1. *Basic Equations*

At a given stage of accretion, the dark star has a prescribed mass. We make the assumption that it can be described as a polytrope in hydrostatic and thermal equilibrium. The hydrostatic equilibrium is defined by

$$\frac{dP}{dr} = -\rho \frac{GM_r}{r^2}; \quad \frac{dM_r}{dr} = 4\pi r^2 \rho(r) \quad (3)$$

and by the polytropic assumption

$$P = K\rho^{1+1/n} \quad (4)$$

where P is the pressure, ρ is the density, M_r is the mass enclosed within radius r, and the constant K is determined once the total mass and radius are specified (Chandrasekhar 1939). Pre-main-sequence stellar models are adequately described by polytropes in the range $n = 1.5$ (fully convective) to $n = 3$ (fully radiative). Given P and ρ at a point, the temperature T is defined by the equation of state of a mixture of gas and radiation

$$P(r) = \frac{R_g \rho(r) T(r)}{\mu} + \frac{1}{3} a T(r)^4 = P_g + P_{rad} \quad (5)$$

where $R_g = k_B/m_u$ is the gas constant, m_u is the atomic mass unit, k_B is the Boltzmann constant, and the mean atomic weight $\mu = (2X + 3/4Y)^{-1} = 0.588$. We take the H mass fraction $X = 0.76$ and the He mass fraction $Y = 0.24$. In the resulting models $T \gg 10{,}000$ K except near the very surface, so the approximation for μ assumes that H and He are fully ionized. In the final models with masses near 800 $M_\odot$ the radiation pressure is of considerable importance.

Given a mass M and an estimate for the outer radius R_*, the hydrostatic structure is integrated outward from the center. At each point $\rho(r)$ and $T(r)$ are used to determine the Rosseland mean opacity κ from a zero-metallicity table from OPAL (Iglesias & Rogers 1996),

supplemented by a table from Lenzuni et al. (1991) for $T < 6000$ K. The photosphere is defined by the hydrostatic condition

$$\kappa P = \frac{2}{3} g \quad (6)$$

where g is the acceleration of gravity. This point corresponds to inward integrated optical depth $\tau \approx 2/3$. When it is reached, the local temperature is set to T_{eff} and the stellar radiated luminosity is therefore

$$L_* = 4\pi R_*^2 \sigma_B T_{\text{eff}}^4 \quad (7)$$

where R_* is the photospheric radius.

The thermal equilibrium condition is $L_* = L_{\text{tot}}$, where the total energy supply for the star (see below) is dominated during the DS phase by the DM luminosity L_{DM}. Thus the next step is to determine L_{DM} from equation (2) and from the density distribution of dark matter (discussed in the next subsection). Depending on the value of L_{DM} compared to L_*, the radius is adjusted, and the polytrope is recalculated. The dark matter heating is also recalculated based on the revised baryon density distribution. The radius is iterated until the condition of thermal equilibrium is met.

2.2. *DM Densities*

The value of the DM density inside the star is a key ingredient in DM heating. We start with a 10^6 $M_\odot$ halo composed of 85% DM and 15% baryons. We take an initial Navarro, Frenk, & White profile (1996; NFW) with a concentration parameter $c = 2$ at $z = 20$ in a standard ΛCDM universe. We note at the outset that our results are *not* dependent on high central DM densities of NFW haloes. Even if we take the initial central density to be a core (not rising towards the center of the halo), we obtain qualitatively the same results of this paper; we showed this in Freese et al (2008b).

Enhanced DM density due to adiabatic contraction: Further density enhancement is required inside the star in order for annihilation to play any role. Paper I recognized a key effect that increases the DM density: adiabatic contraction (AC). As the gas falls into the star, the DM is gravitationally pulled along with it. Given the initial NFW profile, we follow its response to the changing baryonic gravitational potential as the gas condenses. Paper I used a simple Blumenthal method, which assumes circular particle orbits (Blumenthal et al. 1986; Barnes & White 1984; Ryden & Gunn 1987) to obtain estimates of the density. Subsequently Freese et al. (2008b) did an exact calculation using the Young method (Young 1980) which includes radial orbits, and confirmed our original results (within a factor of two). Thus we feel confident that we may use the simple Blumenthal method in our work. We found

$$\rho_\chi \sim 5(\text{GeV}/\text{cm}^3)(n_h/\text{cm}^3)^{0.81}, \quad (8)$$

where n_h is the gas density. For example, due to this contraction, at a hydrogen density of $10^{13}/\text{cm}^3$, the DM density is 10^{11} GeV/cm^3. Without adiabatic contraction, DM heating in the first stars would be so small as to be irrelevant.

Enhanced DM due to accretion: As further gas accretes onto the DS, driving its mass up from $\sim 1M_\odot$ to many hundreds of solar masses, more DM is pulled along with

it into the star. At each step in the accretion process, we compute the resultant DM profile in the dark star by using the Blumenthal et al. (1986) prescription for adiabatic contraction. The DM density profile is calculated at each iteration of the stellar structure, so that the DM luminosity can be determined.

The continued accretion of DM sustains the dark star for $\sim 10^6$ years. Then, unless the DM is supplemented further, it runs out, that is, it annihilates faster than it can be resupplied. At this point the $10^6 M_\odot$ DM halo has a tiny "hole" in the middle that is devoid of DM. One might hope to repopulate the DM by refilling the "hole," but this requires further study. On a conservative note, this paper disregards this possibility. Without any further DM coming into the star (which is now very large), it would contract and heat up to the point where fusion sets in; then the star joins the Main Sequence (MS). This is one possible scenario which we examine in the paper. Alternatively, there is another possible mechanism to replenish the DM in the dark star that may keep it living longer: capture.

Enhanced DM due to capture: At the later stages, the DM inside the DS may be repopulated due to capture (Iocco 2008; Freese et al. 2008c). This mechanism relies on an additional piece of particle physics, scattering of DM particles off the nuclei in the star. Some of the DM particles bound to the $10^6 M_\odot$ DM halo occasionally pass through the DS, and if they lose enough energy by scattering, can be trapped in the star. Then more DM would reside inside the DS and could continue to provide a heat source. This capture process is irrelevant during the initial stages of the DS, and only becomes important once the gas density is high enough to provide a significant scattering rate, which happens when the DS is already quite large ($> 100 M_\odot$). For capture to be significant, there are two assumptions: (1) the scattering cross section must be high enough and (2) the ambient density of DM must be high enough. Regarding the first assumption: Whereas the existence of DS relies only on a standard annihilation cross section (fixed by the DM relic density), the scattering cross section is more speculative. It can vary over many orders of magnitude, and is constrained only by experimental bounds from direct detection experiments (numbers discussed below). Regarding the second assumption: The ambient density is unknown, but we can again obtain estimates using the adiabatic contraction method of Paper 1. Indeed it seems reasonable for the ambient DM density to be high for timescales up to at most tens-hundreds of millions of years, but after that the $10^6 M_\odot$ host for the dark star surely has merged with other objects and the central regions are likely to be disrupted; simulations have not yet resolved this question. Then it becomes more difficult for the DS to remain in a high DM density feeding ground and it may run out of fuel.

We therefore consider two different situations: adiabatic contraction with and without capture; i.e., with and without additional capture of DM at the later stages. In the latter case we focus on "minimal capture," where the stellar luminosity has equal contributions from DM heating and from fusion, as described further below. In both cases, we find the same result: the dark stars continue to accrete until they are very heavy.

2.3. *Evolution*

The initial condition for our simulations is a DS of 3 $M_\odot$, roughly the mass where the assumption of nearly complete ionization first holds. We find an equilibrium solution for this mass, then build up the mass of the star in increments of one solar mass.

We allow surrounding matter from the original baryonic core to accrete onto the DS, with two different assumptions for the mass accretion: first, the variable rate from Tan & McKee (2004) and second, the variable rate from O'Shea & Norman (2007). The Tan/McKee rate decreases from 1.5×10^{-2} $M_\odot$/yr at a DS mass of 3 $M_\odot$ to 1.5×10^{-3} $M_\odot$/yr at 1000 $M_\odot$. The O'Shea/Norman rate decreases from 3×10^{-2} $M_\odot$/yr at a DS mass of 3 $M_\odot$ to 3.3×10^{-4} $M_\odot$/yr at 1000 $M_\odot$. The accretion luminosity arising from infall of material from the primordial core onto the DS is not included in the radiated energy. It is implicitly assumed to be radiated away in material outside the star, for example an accretion disk (McKee & Tan 2008), and in any case, at the large radii involved here, this energy is small compared with the DM annihilation energy.

We remove the amount of DM that has annihilated at each stage at each radius. We continue stepping up in mass, in increments of 1 $M_\odot$, until we reach 1000 $M_\odot$, the Jeans mass of the core (Bromm & Larson 2004) or until all of the following conditions are met: 1) the total mass is less than 1000 $M_\odot$, 2) the dark matter available from adiabatic contraction is used up; 3) nuclear burning has set in, and 4) the energy generation from gravitational contraction is less than 1% of the total luminosity of the star. The last two of these conditions define the zero-age main sequence (ZAMS). The time step is adjusted for each model to give the correct assumed accretion rate. The final mass can be less than 1000 $M_\odot$ because of feedback effects of the ionizing stellar radiation, which can reverse the infall of accreting gas (McKee & Tan 2008). The feedback effect is included in an approximate manner, starting when the surface temperature reaches 50,000 K.

At the beginning of the evolution, the Schwarzschild stability criterion for convection shows that the model is fully convective; thus the polytrope of $n = 1.5$ is a good approximation to the structure. However as more mass is added and internal temperatures increase, opacities drop and, once the model has reached about 100 $M_\odot$, radiative zones start to appear at the inner radii and move outward. Beyond about 300 $M_\odot$ the model is almost fully radiative. The evolutionary calculation takes into account this effect approximately, by gradually shifting the value of n up from 1.5 to 3 in the appropriate mass range. In the later stages of evolution, the constant value $n = 3$ is used.

2.4. *Energy Supply*

The energy supply for the star changes with time and comes from four major sources:

$$L_{\rm tot} = L_{DM} + L_{\rm grav} + L_{\rm nuc} + L_{\rm cap}. \qquad (9)$$

The general thermal equilibrium condition is then

$$L_* = L_{\rm tot}. \qquad (10)$$

The contribution L_{DM} from adiabatically contracted DM dominates the heat supply first. Its contribution

been discussed previously and is given in equation (2). Later, once the adiabatically contracted DM becomes sparse, the other effects kick in: gravity, nuclear burning, and captured DM. We discuss each of these contributions in turn.

2.4.1. Gravity

At the later stages of evolution, when the supply of DM starts to run out, the star adjusts to the reduction in heat supply by contracting. For a polytrope of $n = 3$, the total energy of the star is

$$E_{\text{tot}} = -\frac{3}{2}\frac{GM^2}{R} + E_{\text{th}} + E_{\text{rad}} \qquad (11)$$

where E_{th} is the total thermal energy and the radiation energy $E_{\text{rad}} = \int aT^4 dV$. Using the virial theorem

$$-\frac{3}{2}\frac{GM^2}{R} + 2E_{\text{th}} + E_{\text{rad}} = 0, \qquad (12)$$

we eliminate E_{th} from equation (11) and obtain the gravitational contribution to the radiated luminosity

$$L_{\text{grav}} = -\frac{d}{dt}(E_{\text{tot}}) = \frac{3}{4}\frac{d}{dt}\left(\frac{GM^2}{R}\right) - \frac{1}{2}\frac{d}{dt}E_{\text{rad}}. \quad (13)$$

2.4.2. Nuclear Fusion

Once the star has contracted to sufficiently high internal temperatures $\sim 10^8$K, nuclear burning sets in. For a metal-free star, we include the following three energy sources: 1) the burning of the primordial deuterium (mass fraction 4×10^{-5}) at temperatures around 10^6 K, 2) the equilibrium proton-proton cycle for hydrogen burning, and 3) the triple-alpha reaction for helium burning. At the high internal temperatures (2.75×10^8 K) needed for the star to reach the ZAMS, helium burning is an important contributor to the energy generation, along with the proton-proton cycle. We stop the evolution of the star when it reaches the ZAMS, so changes in abundance of H and He are not considered. Then $L_{\text{nuc}} = \int \epsilon_{\text{nuc}} dM$ where ϵ_{nuc} is the energy generation rate in erg g^{-1} s^{-1}; it is obtained by the standard methods described in Clayton (1968). The astrophysical cross section factors for the proton-proton reactions are taken from Bahcall (1989, Table 3.2), and the helium-burning parameters are taken from Kippenhahn & Weigert (1990).

2.4.3. Feedback

During the initial annihilation phase, the surface temperature T_{eff} remains at or below 10^4 K. However once gravitational contraction sets in, it increases substantially, reaching $\approx 10^5$ K when nuclear burning starts. In this temperature range, feedback effects from the stellar radiation acting on the infalling material can shut off accretion (McKee & Tan 2008). These effects include photodissociation of H$_2$, Lyman α radiation pressure, formation and expansion of an HII region, and photoevaporation of a disk. These effects become important at a mass of ≈ 50 M$_\odot$ in standard Pop III calculations of accretion and evolution, but the effect is suppressed until much higher masses in the DM case because of much lower T_{eff}. Noting that 50 M$_\odot$ on the standard metal-free ZAMS corresponds to $T_{\text{eff}} \approx 50,000$ K (Schaerer 2002), we apply a linear reduction factor to the accretion rate

above that temperature, such that accretion is shut off completely when $T_{\text{eff}} =$100,000 K. This cutoff generally determines the final mass of the star when it reaches the ZAMS.

2.4.4. Capture

The contribution L_{cap} is determined by calculating the annihilation rate of captured DM

$$L_{\text{cap}} = 2m_\chi \Gamma_{\text{cap}}, \qquad (14)$$

where

$$\Gamma_{cap} = \int d^3x \rho_{\text{cap}}^2 \langle \sigma v(r) \rangle / m_\chi \qquad (15)$$

and $\rho_{\text{cap}}(r)$ is the density profile of captured DM. DM heating from captured DM has previously been discussed in detail by Freese et al. (2008c) and Iocco (2008).

The density profile of the captured DM has quite a different shape than the adiabatically contracted (AC) DM density profile discussed previously. Whereas the AC profile is more or less constant throughout most of the star (see Fig. 3), the captured DM profile is highly concentrated toward the center with an exponential falloff in radius, as we will now show. Once DM is captured, it scatters multiple times, thermalizes with the star, and sinks to the center of the star. The DM then assumes the form of a thermal distribution in the gravitational well of the star

$$\rho_{\text{cap}} = m_\chi n_{\text{cap}} = f_{\text{Eq}} f_{\text{Th}} \rho_{\text{o,c}} e^{-[\phi(r)m_\chi/T_c]}. \qquad (16)$$

Here T_c, the star's central temperature, is used since the DM has the same temperature as the stellar core; $\phi(r)$ is the star's gravitational potential; $\rho_{\text{o,c}}$ is the central density of the captured DM; and f_{Th} and f_{Eq} are discussed below. One can immediately see another difference with the AC profile: for captured DM the profile is more centrally concentrated for larger DM particle mass, whereas the density profile for adiabatically contracted DM is independent of particle mass.

The quantity f_{Th} is the probability that a captured DM particle has thermalized with the star.

$$f_{\text{Th}} = 1 - e^{-t_1/\tau_{\text{Th}}}. \qquad (17)$$

t_1 is the time since a DM particle has been captured and τ_{Th} is the thermalization time scale of captured DM.

Captured DM does not immediately thermalize with the star; it requires multiple scatters. The thermalization time scale for the DM is

$$\tau_{\text{Th}} = \frac{m_\chi/m_H}{2\sigma_{\text{sc}} v_{\text{esc}} n_H} \qquad (18)$$

as previously discussed in Freese et al. (2008c). Here v_{esc} is the escape velocity from the surface of the star, n_H is the average stellar density of hydrogen, and m_H is the proton mass. We have only considered spin-dependent scattering, which includes scattering off hydrogen with spin 1/2, but not off Helium which has spin 0.

Heating from captured DM is unimportant until the star approaches the MS; the thermalization time scale is very long (millions of years) and $f_{\text{Th}} \approx 0$. Once the DM supplied from adiabatic contraction runs out, the star begins to contract, and the thermalization time scale becomes very short, on the order of a year. Thus, the star rapidly transitions from $f_{\text{Th}} \approx 0$ to $f_{\text{Th}} \approx 1$. The DM is

either in thermal equilibrium or it is not. With this in mind, t_1 has been set to 100 yrs for all of the simulations. Only $\tau_{\rm Th}$ is recalculated at every time step, which is a reasonable prescription; t_1 set between a few thousand years and a few years makes no quantitative difference upon the evolution of the DS.

The ratio $f_{\rm Eq}$ gives the ratio of DM particles currently inside of the star due to capture, N, to the maximum number of DM particles that could possibly be present, N_o,

$$f_{\rm Eq} = \frac{N}{N_o}. \qquad (19)$$

At the start of the simulation, the DS is too diffuse to capture any DM and $f_{\rm Eq} \approx 0$. Once the star goes onto the main sequence, the maximum number is reached and $f_{\rm Eq} \approx 1$.

We can now give an explicit expression of $f_{\rm Eq}$ by solving for the total number of particles N bound to the star. This number is determined by a competition between capture and annihilation,

$$\dot{N} = C - 2\Gamma, \qquad (20)$$

where 'dot' refers to differentiation in time. The total number of DM particles captured per unit time C was calculated following Gould (1987a). The total number of DM particles annihilated per unit time Γ contains a factor of two since two particles are annihilated per annihilation.). Equation (20) can be solved for N,

$$N = N_o \tanh(t_2/\tau_{eq}) \qquad (21)$$

where $N_o = \sqrt{C/C_A}$, and $\tau_{eq} = 1/\sqrt{CC_A}$, and $C_A = 2\Gamma/N^2$ (Griest & Seckel 1987).

When the annihilation rate equals the capture rate, N goes to N_o. This transition occurs on the equilibrium time scale τ_{eq}. The equilibrium time scale is recalculated at each time step. The time t_2 in equation (21) counts the time since capture is turned on. In equation (16), we now set

$$f_{\rm Eq} = \frac{N}{N_o} = \tanh(t_2/\tau_{eq}). \qquad (22)$$

Conceptually t_2 is not the same as t_1 but at a practical level it is reasonable to set $t_2 = t_1$. In the first place, t_1 refers to the time since a single DM particle has been captured and in fact t_1 is different for each captured DM particle. On the other hand, t_2 is a single time for all captured and thermalized DM and starts when capture turns on. Regardless, once the star descends towards the main sequence, $f_{\rm Eq}$ and $f_{\rm Th}$ both go to unity. The connection is not a coincidence. First τ_{eq} is a factor of a few to a hundred less than $\tau_{\rm Th}$ throughout the simulation. In addition, $t_2 > t_1$ except for the very first DM particle captured. Fixing $t_2 = t_1$ does not change the behavior of $f_{\rm Eq}$ in relation $f_{\rm Th}$ as just described. Hence, for simplicity the simulation assumes $t_1 = t_2$.

In the limit that $f_{\rm Eq}$ and $f_{\rm Th}$ go to unity, then $\Gamma_{cap} = C/2$. Hence, $L_{\rm cap}$ simplifies to

$$L_{\rm cap} = \frac{2}{3} m_\chi C \qquad (23)$$

where the 2/3 accounts for the loss of neutrinos as previously discussed in connection with equation (2). Also roughly $L_{\rm cap} \propto \bar{\rho}_\chi \sigma_{sc}$ and is independent of m_χ. Hence

$L_{\rm cap}$ scales with both the ambient background DM density $\bar{\rho}_\chi$, and the scattering cross section of the DM off of baryons $\sigma_{\rm sc}$.

Physically reasonable values for the scattering cross section and background DM densities imply that $L_{\rm cap}$ can affect the first stars once they approach the MS. Direct and indirect detection experiments require $\sigma_{sc} \leq 4 \times 10^{-39}$ (Savage et al. 2004; Chang et al. 2008; Savage et al 2008; Hooper et al. 2009); a WIMP's σ_{sc} can be many orders of magnitude smaller than the experimental bound. The ambient background DM density, $\bar{\rho}_\chi$, can be very high, on the order of $10^{14} ({\rm GeV/cm}^3)$ (as obtained from Eq. (8)) due to adiabatic contraction. To demonstrate the "minimal" effect of capture, we set $\bar{\rho}_\chi = 1.42 \times 10^{10} ({\rm GeV/cm}^3)$ and $\sigma_{sc} = 10^{-39} {\rm cm}^2$, chosen so that about half of the luminosity is from DM capture and the other half from fusion for the standard 100 GeV case at the ZAMS. These parameters have been used in all cases where capture has been turned on. Even minimal capture shows that DM capture lowers the star's surface temperature and increases the mass of the first stars.

We note that the product of ambient density and cross section could be very different than the values used in this paper. If this product is much smaller than the values considered in the 'minimal capture' case, then fusion completely dominates over capture and one may ignore it. On the other hand, if this product is much larger than the 'minimal capture' case, then fusion is negligible and the DS may continue to grow by accretion and become much larger than discussed in this paper; this case will be discussed elsewhere. The 'minimal' case is thus the borderline case between these two possibilities, and lasts only as long as the DS remains embedded in a high ambient DM density assumed here.

3. RESULTS

Here we present our results for the evolution of a DS, starting from a $3M_\odot$ star powered by DM annihilation (defined as $t = 0$), building up the stellar mass by accretion, and watching as the other possible heat sources become important. We have considered a range of DM masses: 1 GeV, 10 GeV, 100 GeV, 1 TeV and 10 TeV, which characterizes the plausible range for WIMP masses. Since the DM heating scales as $\langle \sigma v \rangle / m_\chi$, this range of particle masses also corresponds to a range of annihilation cross sections. To account for the uncertainties associated with the accretion rate, the study has used two different accretion rates: one from Tan & McKee (2004) and the other from O'Shea & Norman (2007) (as discussed in section 2.3 above). We consider the case of (i) no capture and (ii) "minimal capture" (defined as above), with $\bar{\rho}_\chi = 1.42 \times 10^{10} ({\rm GeV/cm}^3)$ and $\sigma_{sc} = 10^{-39} {\rm cm}^2$, chosen so that about half of the luminosity is from DM capture and the other half from fusion for the standard 100 GeV case at the ZAMS. In this paper we will not treat the case of maximal capture, where the DM heating would dominate (over all other sources including fusion) so that the DS would continue to grow as long as it is fed more DM.

We here show the results of our simulations. First we briefly outline our results and present our tables and figures. These are then discussed in detail, case by case, in the remainder of the results section.

TABLE 1
PROPERTIES AND EVOLUTION OF DARK STARS FOR $m_\chi = 1$ GeV, $\dot{M}$ FROM TAN & MCKEE, $\langle \sigma v \rangle = 3 \times 10^{-26}$ CM^3/S. FOR THE LOWER STELLAR MASSES, IDENTICAL RESULTS ARE OBTAINED FOR THE CASES OF NO CAPTURE AND MINIMAL CAPTURE; HENCE THE FIRST FOUR ROWS APPLY EQUALLY TO BOTH CASES. THE FIFTH AND SIXTH ROWS APPLY ONLY TO THE NO CAPTURE CASE WHILE THE LAST TWO ROWS APPLY ONLY WHEN CAPTURE IS INCLUDED.

M_* ($M_\odot$)	L_* ($10^6 L_\odot$)	R_* (10^{12}cm)	$T_{\rm eff}$ (10^3K)	ρ_c (gm/cm^3)	T_c (10^6K)	M_{DM} (10^{31}g)	$\rho_{\rm o,DM}$ (gm/cm^3)	t (10^3yr)
106	9.0	240	5.4	1.8×10^{-8}	0.1	36	4.5×10^{-11}	19
371	17	270	5.9	5.2×10^{-8}	0.20	64	2.0×10^{-11}	119
690	6.0	110	7.5	5.9×10^{-6}	1.0	10	6.8×10^{-11}	280
756	3.3	37	10	2.2×10^{-4}	3.4	1.2	4.8×10^{-10}	310
793	4.5	5.1	31	8.9×10^{-2}	25	≈ 0.0	≈ 0.0	330
820	8.4	0.55	111	115	276	≈ 0.0	≈ 0.0	430
Alternative properties for final two masses with capture included:								
793	4.6	5.7	30	7.1×10^{-2}	24	8.4×10^{-4}	2.94×10^{-8}	328
824	8.8	.58	109	102	265	8.1×10^{-5}	2.14×10^{-6}	459

TABLE 2
PROPERTIES AND EVOLUTION OF DARK STARS FOR $m_\chi = 100$ GeV, $\dot{M}$ FROM TAN & MCKEE, $\langle \sigma v \rangle = 3 \times 10^{-26}$ CM^3/S. ENTRIES AS DESCRIBED IN TABLE 1.

M_* ($M_\odot$)	L_* ($10^6 L_\odot$)	R_* (10^{12}cm)	$T_{\rm eff}$ (10^3K)	ρ_c (gm/cm^3)	T_c (10^6K)	M_{DM} (10^{31}g)	$\rho_{\rm o,DM}$ (gm/cm^3)	t (10^3yr)
106	1.0	70	5.8	1.1×10^{-6}	0.4	16	1.8×10^{-9}	19
479	4.8	84	7.8	2.0×10^{-5}	1.4	41	2.0×10^{-9}	171
600	5.0	71	8.5	4.1×10^{-5}	1.8	36	1.9×10^{-9}	235
716	6.7	11	23	2.0×10^{-2}	15	2.7	3.8×10^{-8}	303
756	6.9	2.0	56	2.8	78	≈ 0.0	≈ 0.0	330
779	8.4	0.55	110	120	280	≈ 0.0	≈ 0.0	387
Alternative properties for final two masses with capture included:								
756 (c)	6.8	2.0	55	2.55	76	7.5×10^{-5}	5.3×10^{-5}	328
787(c)	8.5	0.58	108	105	270	2.2×10^{-5}	5.3×10^{-4}	414

TABLE 3
PROPERTIES AND EVOLUTION OF DARK STARS FOR $m_\chi = 10$ TeV, $\dot{M}$ FROM TAN & MCKEE, $\langle \sigma v \rangle = 3 \times 10^{-26}$ CM^3/S. ENTRIES AS DESCRIBED IN TABLE 1.

M_* ($M_\odot$)	L_* ($10^6 L_\odot$)	R_* (10^{12}cm)	$T_{\rm eff}$ (10^3K)	ρ_c (gm/cm^3)	T_c (10^6K)	M_{DM} (10^{31}g)	$\rho_{\rm o,DM}$ (gm/cm^3)	t (10^3yr)
106	0.1	22	6.0	3.8×10^{-5}	1.3	7.8	1.8×10^{-8}	19
310	0.59	21	9.3	4.4×10^{-4}	3.6	15	1.5×10^{-7}	88
399	3.3	6.6	25	3.6×10^{-2}	16	6.6	9.9×10^{-7}	134
479	3.0	2.9	32	0.5	40	2.1	1.1×10^{-6}	172
552	5.2	0.56	97	79	220	≈ 0.0	≈ 0.0	230
552	5.3	0.47	107	136	270	≈ 0.0	≈ 0.0	256
Alternative properties for final two masses with capture included:								
550 (c)	5.2	0.6	95	66	210	8.5×10^{-12}	5.3×10^4	230
553 (c)	5.4	0.48	105	127	260	5.7×10^{-12}	1.2×10^5	266

Tables 1–3, each for a fixed m_χ, present the evolution of some basic parameters of the star throughout the DS phase: stellar mass M_*, luminosity L_*, photospheric radius R_*, surface temperature $T_{\rm eff}$, the star's baryonic central density ρ_c, central temperature T_c, the amount of DM inside of the star $M_{\rm DM}$, the DM's central density $\rho_{\rm o,DM}$, as well as the elapsed time t since the start of the calculation. $M_{\rm DM}$ and $\rho_{\rm o,DM}$ give the mass and density of DM either from adiabatic contraction (the first 6 rows) or from capture (the last two rows).

In the tables, the stellar masses were chosen to roughly characterize important transitions for the DS. The first mass was chosen at roughly the time when a dark star begins to take on the size, temperature, and luminosity which are characteristic of the DS phase, which is around 100 $M_\odot$. The second mass is given when the DS acquires its maximum amount of DM, which varies from case to case. The third mass is towards the end of the DS adiabatic phase. The fourth row characterizes the star's properties just prior to running out of adiabatically contracted DM. The fifth row is given just after the star runs out of adiabatically contracted DM, while the sixth gives the star's properties on the ZAMS. Capture only becomes important once the adiabatically contracted DM has run out. Prior to running out, the stellar evolution is the same with or without DM capture. For the case with capture included, the seventh and eighth row should be used instead of the fifth and sixth row.

Further features of the calculations are shown in Figures 1–4, which give, respectively, (1) the evolution of all cases without capture in the Hertzsprung-Russell diagram, (2) the luminosity as a function of time for the 100 GeV case with and without capture, (3a) the evolution of the density distribution of the baryonic and dark matter for the 100 GeV case without capture, (3b) the distribution of dark matter heating rate for the 100 GeV case with capture, and (4) the evolution of various quantities for all cases without capture.

3.1. *Canonical Case without Capture*

Our canonical case takes $m_\chi = 100$ GeV, the accretion rate as given by Tan & McKee (2004), and $\langle \sigma v \rangle = 3 \times 10^{-26}$ cm^{3}s^{-1} for the calculation of the annihilation rate.

The initial model (defined to be $t = 0$) has a mass of 3 $M_\odot$ with a surface temperature of 4100 K, a radius of 3×10^{13} cm, a luminosity of 4.5×10^4 $L_\odot$ and a fully convective structure. The DS stays fully convective for stellar masses below 50 $M_\odot$ at which point a small radiative zone appears. The star makes a transition from convective to radiative in the $M_* = (100-200)$ $M_\odot$ mass range, with a radiative zone growing outward from the center, and then becomes fully radiative (but for a small convective region at the surface) for $M_* > 300$ $M_\odot$. The star stays almost fully radiative for the remainder of the DS phase. Above 750 $M_\odot$, hydrogen and helium burning set in, and a new convective zone appears at the center of the star.

Evolution of Dark Matter Density: The DM densities inside of the star change due to annihilation and the evolution of the dark star's baryonic structure. Figure 3 plots the baryonic and DM density profiles for the standard case at several different stellar masses. As the star's mass grows, the DM and baryonic densities also increase. The DM profile for the last model, which has a stellar

mass of 779 $M_\odot$, is not plotted because at this point all of the adiabatically contracted DM has been used up.

The adiabatically contracted DM density profile is more or less constant with radius and then falls off toward the surface of the star. The DM densities for the earlier models show a density increase toward the center of the star due to the original NFW profile, e.g. in the 300 $M_\odot$ model. The slight peak flattens out at higher stellar masses as can be seen in the 500 $M_\odot$ models, since regions with a higher DM density annihilate more rapidly than regions with a lower DM density. Once the peak is worn away, the central DM profile stays flat and ultimately decreases.

The DM and baryonic densities evolve slowly for much of the DS phase. In fact between 100 $M_\odot$ and 600 $M_\odot$, the DM central density barely changes (Table 2). Initially, the DM mass grows (Fig. 4e) and reaches a maximum when the total mass is about 450 $M_\odot$, at which point the star has about 0.2 $M_\odot$ of DM. At this point, the DM heating becomes insufficient to support the star. The star begins to slowly contract and boosts the DM density, but the boost is still modest up to a time of 2×10^5 years or until the star reaches 600 $M_\odot$.

Around 600 $M_\odot$, the star begins to rapidly shrink. Note the rapid dominance of gravitational energy at this time (Fig. 2). The DM densities shoot up, but the total amount of DM inside of the star precipitously drops. By 750 $M_\odot$, the DM has run out and the star begins to transition into a standard Pop. III star. The star reaches the MS at around 780 $M_\odot$ at which point feedback effects cut off any further accretion.

Evolution of temperature and energy generation: The surface properties of the DS evolve rapidly between the initial model at 3 $M_\odot$ and 100 $M_\odot$. The luminosity shoots up by a factor of 25, the radius by a factor of 3, and the star's surface temperature goes from 4100 K to 5800 K.

The star looks radically different from a metal-free star on the MS. Even at 100 $M_\odot$, the DS is still very cool with a surface temperature of around 5800 K vs 100,000 K (for the standard ZAMS) and has a central temperature of only about a half a million degrees Kelvin vs 200 million degrees (ZAMS). The star is also much more extended, $\approx 7 \times 10^{13}$ cm vs $\approx 5 \times 10^{11}$ cm (ZAMS).

Between $100 - 600$ $M_\odot$, the star's luminosity evolves less rapidly, increasing by a factor of 5 to a value of 5×10^6 $L_\odot$. The star's surface temperature reaches 7800 K, while the radius remains almost constant, passing through a broad maximum at about 8.5×10^{13} cm. The central temperature is still quite cool (1.8×10^6 K) compared to a metal-free ZAMS star. Most of the star is still too cool to even burn deuterium and lithium. DM continues to power the star, as is apparent in Figure 2.

Above 600 $M_\odot$, the DS begins to transform into a standard metal-free star. As the DM begins to run out the surface temperature begins to shoot up and the stellar radius shrinks. Just prior to running out of DM, at 716 $M_\odot$, the star's surface reaches 23,000 K, the radius has shrunk to 10^{13} cm and the central temperature has shot up to 15 million K. Near the beginning of this rapid contraction the star is sufficiently hot to burn deuterium rapidly, as can be seen from the spike of nuclear heating in Figure 2 just before 0.3 Myr; this spike lasts about 50,000 years. The burning of deuterium, however, remains an insignifi-
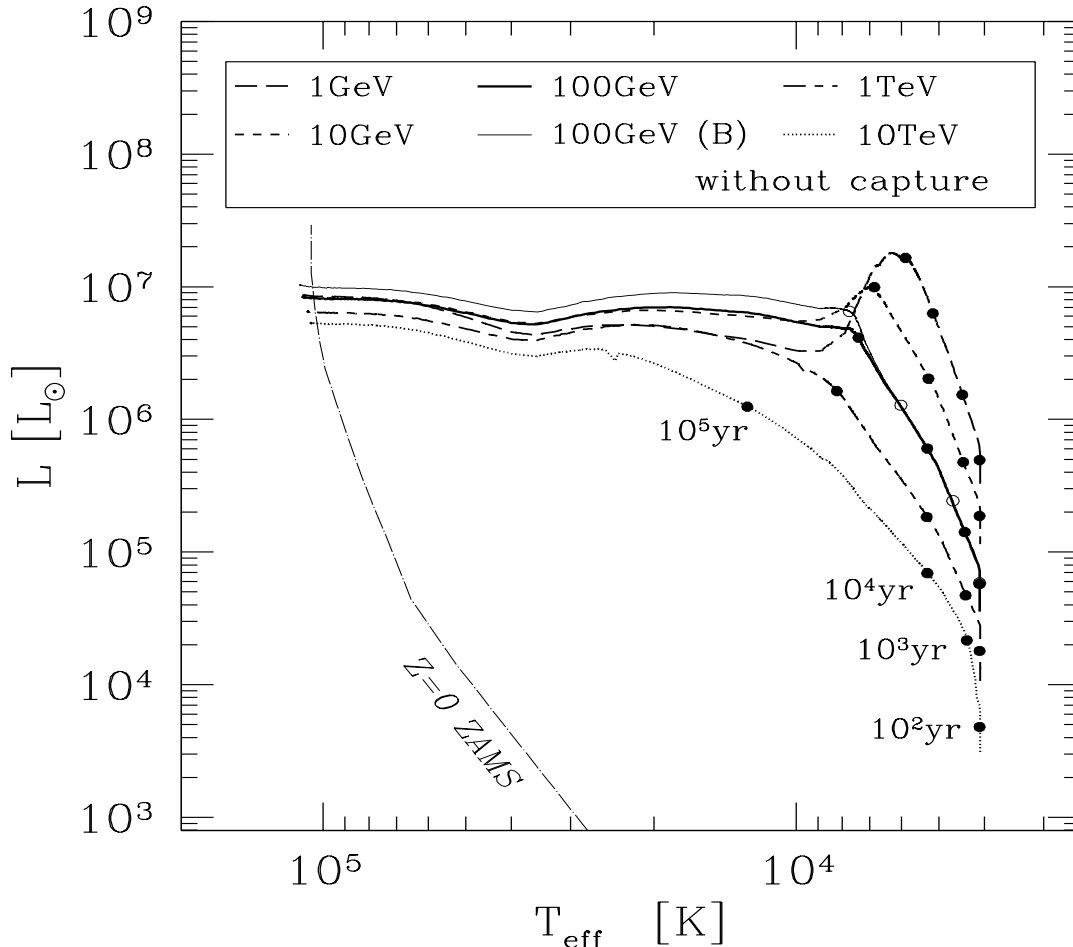
FIG. 1.— Evolution in the H-R diagram, for 5 different particle masses as indicated in the legend. The luminosity is given in solar units and the temperature is in Kelvin. The dots indicate a series of time points, which are the same for all cases. The open dots distinguish the 100 GeV (B) case from the 100 GeV case. All cases are calculated with the accretion rate given by Tan & McKee (2004) except the curve labelled 100 GeV (B), which is calculated with the rate given by O'Shea & Norman (2007). The metal-free zero-age main sequence ($Z = 0$ ZAMS) is taken from Schaerer (2002). The peak below 10^4K in the 1 GeV case is due to the overwhelming DM luminosity in this case.

cant power source for the star. As the DS runs out of DM gravity and nuclear burning begin to turn on as energy sources for the star. Just at the point where all three energy sources (DM heating, gravity, and nuclear burning) all contribute simultaneously, the luminosity increases by about 50 % and then decreases again; one could call this a "flash" which lasts about 20,000 years and is the "last gasp" of adiabatically contracted DM annihilation.

Near 750 M$_\odot$ the energy generation in the star becomes dominated by, first, gravity, and then nuclear burning. The star's surface temperature is just above 50,000 K (Table 2) and feedback effects have started to cut off the accretion of baryons. Eventually, the star begins to settle onto the MS and nuclear burning becomes the dominant power source. The surface temperature has shot up to 109,000 K, and finally feedback effects have stopped any further accretion. On the MS, the radius is 5.5×10^{11} cm and the central temperature has gone up to 280 million K. At the final cutoff, which is our zero-age main sequence model, the star has a mass of 779 M$_\odot$.

The final model on the metal-free MS compares well with that produced by a full stellar structure code (Schaerer 2002). Schaerer's radius is slightly larger at 8.4×10^{11} cm vs. 5.5×10^{11} cm for the polytrope. The

polytrope's surface temperature is slightly too high at 109,000 K vs 106,000 K and the polytrope's luminosity is too low by a factor of about 2. The difference is not surprising; we have not done the radiative energy transport. Remarkably, the numbers are quite close despite the polytropic assumption.

3.2. General Case without Capture

In addition to the canonical case, we have studied many other parameter choices as described previously: a variety of WIMP masses (or, equivalently, annihilation cross sections) and a variety of accretion rates. In this section we still restrict ourselves to the case of no capture. In all cases, we obtain the same essential results. While one can see in Figure 4 that there is some scatter of the basic properties of the star, yet we find the following general results for all cases: DS evolution occurs over an extended period of time ranging from $(2-5) \times 10^5$ years. All cases have an extended radius $(2 \times 10^{13} - 3 \times 10^{14})$cm, are cool ($T_{\rm eff} < 10,000$ K) for much of the evolution, and have a large final mass $(500 - 1000)$ M$_\odot$. All of the DS cases studied are physically very distinct from standard Pop. III stars. The standard Pop. III star is physically more compact with a radius of only $\approx 5 \times 10^{11}$cm, and
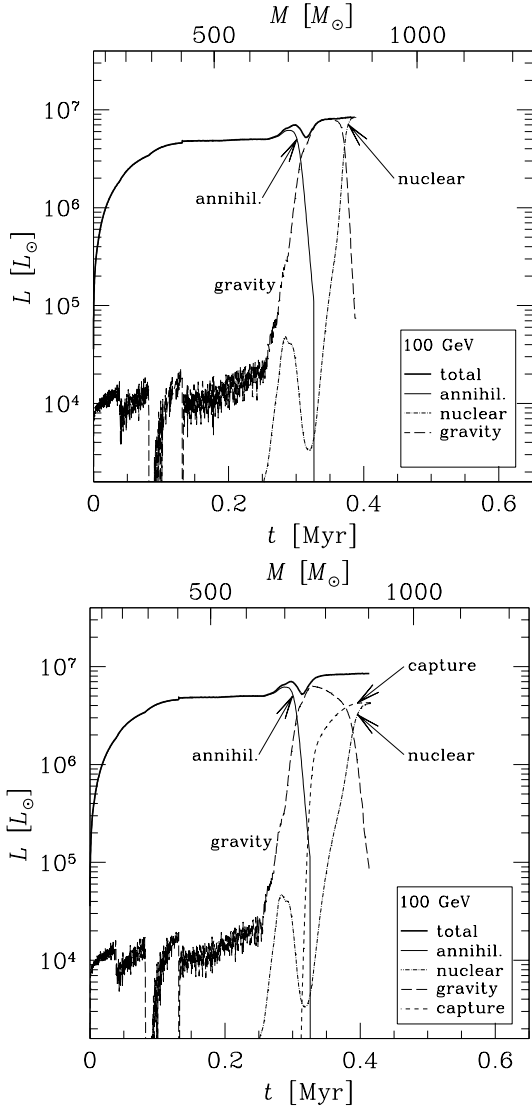
FIG. 2.— Luminosity evolution for the 100 GeV case as a function of time (*lower scale*) and stellar mass (*upper scale*). The solid (red) top curve is the total luminosity. The lower curves give the partial contributions of different sources of energy powering the star a) (*upper frame*) without capture, and b) (*lower frame*) with 'minimal' capture. In both frames, the total luminosity is initially dominated by DM annihilation (the total and annihilation curves are indistinguishable until about 0.3 Myr after the beginning of the simulation); then gravity dominates, followed by nuclear fusion. In the lower frame, capture becomes important at late times.

hotter with a surface temperature of ≈100,000 K. The estimated final mass for the standard Pop III.1 star is also smaller, ≈ 100 $M_\odot$, because the high surface temperature leads to radiative feedback effects that prevent accretion beyond that point (McKee & Tan 2008).

Figure 1 shows the evolution curves in the H-R diagram for a variety of cases. The figure shows the evolution for various particle masses with the Tan/McKee accretion rate, and compares the 100 GeV case with a calculation using the O'Shea/Norman accretion rate.

The DS evolution curves on the HR diagram are qualitatively similar for all of the different cases. The DS spends most of its lifetime at low temperatures below 10,000 K. Eventually, DM begins to run out, the star contracts and heats up, and gravity and nuclear burning begin to turn on. Just at the point where all three
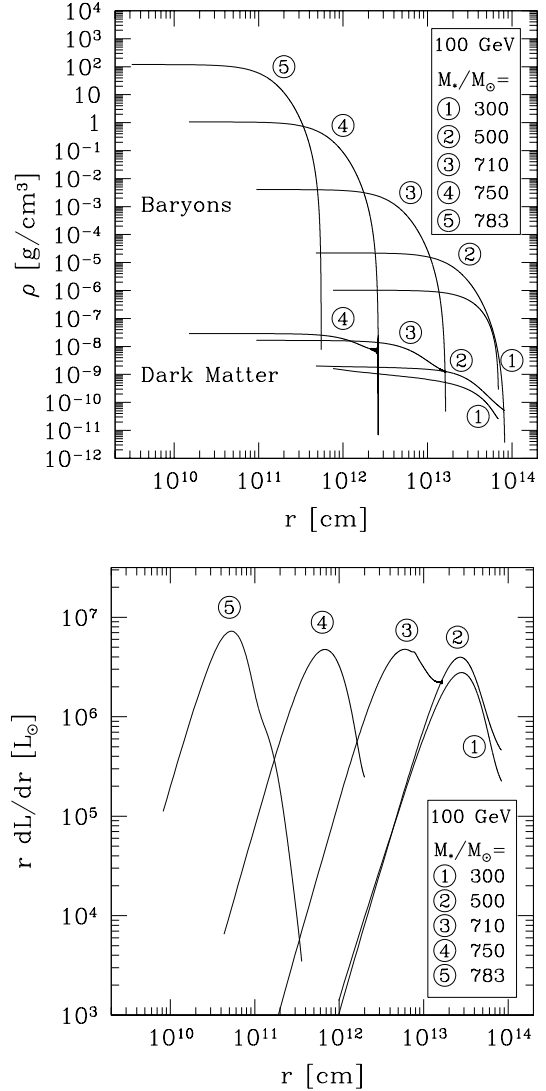

FIG. 3.— a) (*upper frame*): Evolution of a dark star for $m_\chi = 100$ GeV as mass is accreted onto the initial protostellar core of 3 $M_\odot$ (for the case of no capture). The set of upper (lower) solid curves correspond to the baryonic (DM) density profile (values given on left axis) at different stellar masses and times. b)(*Lower frame*): differential luminosity rdL_{DM}/dr as a function of r for the masses indicated.

power sources are important, the luminosity "flashes" (as seen in Fig. 2), i.e., increases by a 50 % for about 20,000 years and then goes back down. Then, DM runs out. For the lower particle masses, as seen in Fig. 1, the luminosity drops slightly as gravity becomes the main and dominant power source. As the surface temperature continues to increase, nuclear burning becomes important when $T_{eff} \approx 30,000$ K. Above this temperature (see Fig. 1), the stellar luminosity again increases as the star approaches the ZAMS. Above 50,000 K, feedback effects turn on and begin to stop the accretion of baryons. Once the star reaches 100,000 K, accretion completely stops, and the star goes onto the ZAMS.

While the basic DS evolution is similar for all cases, we now discuss the variation due to different parameters. The evolution curves differ depending upon the DM particle mass. For larger m_χ, the stellar mass and luminosity decrease such that the evolution curve on the
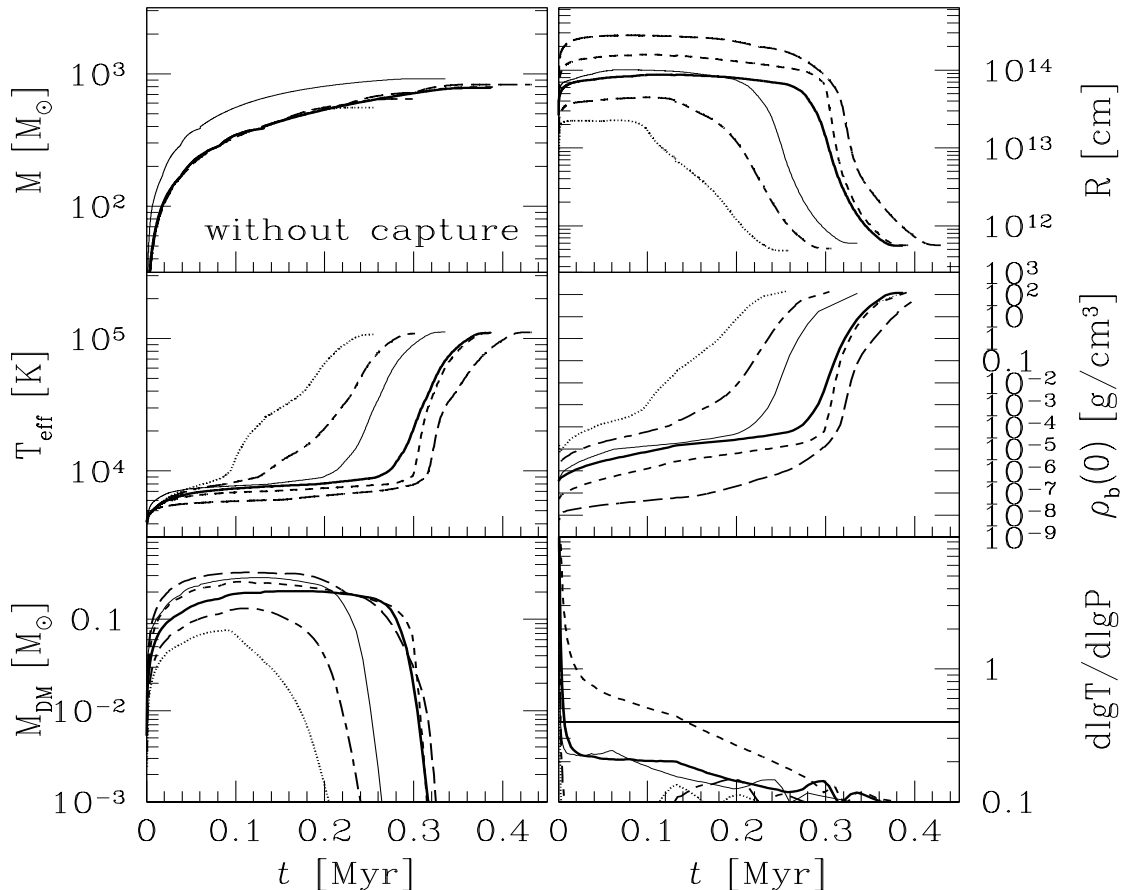
Fig. 4.— Dark Star evolution (for the case of no capture) illustrating dependence on DM particle mass and accretion rate(O'Shea/Norman vs. Tan/McKee). Different curves are the same as explained in the legend of Fig. 1. The quantities plotted are a) stellar mass (*upper left*), b) total radius (*upper right*), c) surface temperature (*middle left*), d) central stellar (baryon) density (*middle right*), e) amount of DM inside of the star (*lower left*), and f) radiative gradient at the center of the star (*lower right*). In the latter plot, central regions above the horizontal line are unstable to convection; hence this plot illustrates the onset of a central radiative zone.

H-R diagram for the 1 TeV case is beneath that for the 100 GeV case. The reduced luminosity is a consequence of the reduced energy production at the higher particle masses, since DM heating is inversely proportional to m_χ (see eq. (1)). Then at higher particle masses a smaller radius is needed to balance the dark-matter energy production and the radiated luminosity.

In the Tables and in Figure 3, one can see the density profiles of the various components in the DS. The DM densities also depend upon m_χ. As shown in the Tables, the average DM density in the star is an increasing function of m_χ. For example, at the time the DS reaches 100 $M_\odot$, the central DM densities vary between 2×10^{-8} g/cm^3 for $m_\chi = 10$ TeV and 5×10^{-11} g/cm^3 for $m_\chi = 1$ GeV. These densities are many orders of magnitude lower than the baryon densities in the DS, as can be seen in Figure 3. Here one can see "the power of darkness:" Despite the low DM densities in the star, DM annihilation is an incredibly efficient energy source since nearly all of the particle mass is converted to heat for the star. We also wish to point out that both baryon and DM densities in the DS are far lower than in metal free main sequence stars of similar stellar mass; ZAMS stars have densities > 1 gm/cm^3.

One can also see the dependence of the DS evolution

upon accretion rate. Our canonical case, obtained using the accretion rate from Tan & McKee (2004), can be contrasted with that using the O'Shea/Norman accretion rate. For 100 GeV particles, the DS evolution is identical for the two accretion rates until $T_{\rm eff} \sim 7,000$ K (10^5 yr). After that the luminosity of the O'Shea/Norman case shoots higher as a result of the higher accretion rate. Consequently the DS with the O'Shea/Norman accretion rate has a shorter lifetime than the DS with the Tan/McKee accretion rate (350 vs. 400 thousand years); a larger final mass (916$M_\odot$ vs. 780$M_\odot$) and higher luminosity.

The 1 GeV case displays some interesting behavior: one can see a spike in the evolutionary track on the H-R diagram. The DS reaches a maximum luminosity of 2×10^7 L$_\odot$ and then subsequently drops by a factor of nearly ten, crossing beneath the 100 GeV case. Subsequently the 1 GeV curve then again crosses the 100 GeV case before settling onto the MS. The large early luminosity is due to extreme effectiveness of DM heating for the 1 GeV case; DM heating is inversely proportional to m_χ (eq. 1).

The stellar structure of all of the cases studied is similar to our canonical case, but the transition from a convective to a radiative structure happens at different times,

depending upon the DM particle mass. The lower right panel in Fig. 4 plots the temperature gradient in the innermost few zones at the center of the DS, to show the onset of radiative energy transfer at the center of the star. Models above the line have convective cores while models below have radiative cores. As we increase the DM mass, the onset of radiative transport happens earlier, at lower stellar masses. For our canonical 100 GeV case, a small radiative zone appears when the mass of the DS reaches $50M_\odot$. The $m_\chi = 1$ GeV case, however, does not begin to form a radiative zone until the mass is nearly 400 $M_\odot$. The larger radii and cooler internal temperatures, compared with the canonical 100 GeV case, result in higher interior opacities, favoring convection.

The timing of the transition from convective to radiative can be understood from the stellar structure. For m_χ greater than the canonical case, the DM heating is less effective since it is inversely proportional to m_χ. The star compensates by becoming more compact, thereby increasing the DM density and the internal temperature. In the relevant temperature range, the opacity scales as $\rho T^{-3.5}$, and ρ scales as T^3. The smaller radius actually results in a decrease in luminosity as well, so the radiative gradient

$$\frac{\mathrm{d}\log T}{\mathrm{d}\log P} = \frac{3\kappa LP}{16\pi GacT^4 M_r} \qquad (24)$$

is reduced, tending to suppress convection relatively early. Conversely if m_χ is less than 100GeV, the star must be more puffy, which increases the radiative gradient. Thus the transition will occur at a later stage.

The cases studied have some differences in terms of lifetime, luminosity, and final mass. At the time the DS has grown to 100 $M_\odot$, the 1 GeV case is an order of magnitude brighter than the 100 GeV case. Similarly, the 100 GeV case is about an order of magnitude brighter than the 10 TeV case. The DS lifetime grows shorter for increasing m_χ. The lifetime for the 1 GeV case is 4.3×10^5 years while the lifetime for the 10 TeV case is only 2.6×10^5 years. The reduced amount of fuel available in the 10 TeV case more than compensates for the lower luminosity in determining the lifetime. Also, the 1 GeV case has a higher final mass than the 10 TeV case (820 $M_\odot$ vs 552 $M_\odot$); clearly a longer lifetime allows more mass to accrete.

3.3. *DM Evolution-Adiabatic Contraction Only*

Here we discuss the evolution of the DS once its DM fuel begins to run out. In this section, we do not consider capture; in the next section we will add the effects of capture as a mechanism to refuel the DM inside the star.

Initially, as baryons accrete onto the DS, adiabatic contraction pulls DM into the star at a sufficiently high rate to support the star, but eventually, adiabatic contraction fails to pull in enough DM at high enough densities to support it.

Adiabatic contraction eventually fails for two main reasons. DM must be brought inside the star, first, to replace the DM which has annihilated away and, second, to support an ever-increasing stellar luminosity as the stellar mass increases due to accretion. In fact, an accretion rate that decreases as a function of time (Tan & McKee 2004) only compounds the problem, leading to a relatively shorter life span since even less DM is brought into the star. With an insuffient amount of DM at high enough densities, the star must contract to increase the DM heating rate to match the stellar luminosity. The contraction leads to higher surface temperatures such that feedback radiative effects eventually shut off accretion altogether.

As the star contracts, a large fraction of DM previously inside of the star ends up outside of the star. The star's contraction amounts to at least two orders of magnitude in radius, leaving a large fraction of the DM outside the star. Thus DM annihilation accounts for only a fraction of the DM "lost" from the star. For instance in the 100 GeV case, only a fifth of the DM is lost due to annihilation; the rest is "left outside".

The "left outside" effect can be understood in a simple way. DM heating is mainly a volume effect as can be seen in Figure 3. Due to adiabatic contraction, ρ_{DM} does not scale perfectly with baryon density (eq. 8). For instance, the total amount of DM inside of star of fixed mass (even without DM annihilation) decreases as the radius of the star shrinks.

Without a way to replenish the DM such as with capture, the DS will eventually run out of DM due to the combination of the "left outside" effect and DM annihilation.

3.4. *DS evolution with Capture included*

The DM inside the DS can be replenished by capture. DM particles bound to the larger halo pass through the star, and some of them can be captured by losing energy in WIMP/nucleon scattering interactions. We remind the reader that we have defined our case of 'minimal capture' to have background DM density $\bar{\rho}_\chi = 1.42 \times 10^{10}(\mathrm{GeV/cm^3})$ and scattering cross section $\sigma_{sc} = 10^{-39}\mathrm{cm}^2$ chosen so that about half of the luminosity is from DM capture and the other half from fusion for the standard 100 GeV case at the ZAMS.

With capture, the stellar evolution is the same as in the cases previously discussed without capture throughout most of the history of the DS. The contribution to the heating from capture L_{cap} only becomes important once DM from adiabatic contraction runs out. Once this happens, gravity still initially dominates, but for the 'minimal capture' case we have considered, L_{cap} is more important than L_{nuc} until the star eventually reaches a new "dark" main sequence, where the two contributions become equal. During this phase the star is more extended and cooler than without capture, which allows for more baryons to accrete onto the star once the first dark star phase driven by adiabatic contraction ends. However for the standard minimal case the final mass with capture is at most 1% larger than that without.

In a future paper we will consider the case of much higher capture rates than the minimal ones we have studied here. The capture rate depends on the ambient DM density in which the DS is immersed and on the WIMP/nucleus scattering cross section. High ambient density could easily arise; in fact the adiabatic contraction arguments applied to the DS from the beginning indicate that this is quite likely. On the other hand, the scattering cross section may be significantly lower than the current experimental bound adopted in our minimal capture case. In any case, with a sufficiently high capture rate, say two or more orders of magnitude higher than

the minimal value considered here, the star can stay DM powered and sufficiently cool such that baryons can in principle continue to accrete onto the star indefinitely, or at least until the star is disrupted. This latter case will be explored in a separate paper where it will be shown that the dark star could easily end up with a mass on the order of several tens of thousands of solar masses and a lifetime of least tens of millions of years.

4. DISCUSSION

We have followed the growth of equilibrium protostellar Dark Stars (DS), powered by Dark Matter (DM) annihilation, up to the point when the DS descends onto the main sequence. Nuclear burning, gravitational contraction, and DM capture are also considered as energy sources. During the phase when dark-matter heating dominates, the objects have sizes of a few AU and central $T \approx 10^5 - 10^6$ K. Sufficient DM is brought into the star by contraction from the DM halo to result in a DS phase of at least several hundred thousand years (without DM capture). Because of the relatively low $T_{\rm eff}$ (4000–10,000 K), feedback mechanisms for shutting off accretion of baryons, such as the formation of HII regions or the dissociation of infalling H_2 by Lyman-Werner photons, are not effective until DM begins to run out. The implication is that main-sequence stars of Pop. III are very massive. Regardless of uncertain parameters such as the DM particle mass, the accretion rate, and scattering, DS are cool, massive, puffy and extended. The final masses lie in the range 500–1000 $M_\odot$, very weakly dependent on particle masses, which were assumed to vary over a factor of 10^4.

One may ask how long the dark stars live. If there is no capture, they live until the DM they are able to pull in via adiabatic contraction runs out; the numerical results show lifetimes in the range 3×10^5 to 5×10^5 yr. If there is capture, they can continue to exist as long as they reside in a medium with a high enough density of dark matter to provide their entire energy by scattering, capture, and annihilation.

In addition, the properties of the DM halo affect the nature of the DS. For instance, a larger concentration parameter allows for more DM to be pulled in by adiabatic contraction. The additional DM prolongs the lifetime of the DS phase and increases the DS final mass. The canonical case with a concentration parameter c = 3.5 rather than x = 2 has a final mass of 870 $M_\odot$ vs. 779 $M_\odot$ and has a lifetime of 442,000 yrs vs. 387,000 yrs. Furthermore, the concentration parameter of each DS halo will be different, depending upon the history of each halo. Thus the Initial Mass Function (IMF) of the ZAMS arising from the growth of dark stars will be sensitive to the halo parameters. This effect will be studied thoroughly in a separate publication.

DS shine with a few $10^6 L_\odot$ and one might hope to detect them, particularly those that live to the lowest redshift ($z = 0$ in the most optimistic case). One may hope that the ones that form most recently are detectable by JWST or TMT and differentiable from the standard metal-free Pop. III objects. DS are also predicted to have atomic hydrogen lines originating in the warmer photo-spheres, and H_2 lines arising from the infalling material, which is still relatively cool.

The final fate of DS once the DM runs out is also different from that of standard Pop III stars, again leading to different observable signatures. Standard Pop III stars are thought to be $\sim 100 - 200 M_\odot$, whereas DS lead to far more massive MS stars. Heger & Woosley (2002) showed that for $140 M_\odot < M < 260 M_\odot$, pair instability supernovae lead to odd-even effects in the nuclei produced, an effect that is not observed. Thus if Pop III.1 stars are really in this mass range one would have to constrain their abundance. Instead, we find far more massive Dark Stars which would eventually become heavy main sequence (ZAMS) stars of 500-1000 $M_\odot$. Heger & Woosley find that these stars after relatively short lifetimes collapse to black holes. Or, if they rotate very rapidly, Ohkubo et al (2006) argue that they could become supernovae, leaving behind perhaps half their mass as black holes. In this case the presumed very bright supernova could possibly be observable. In either case, the elemental abundances arising from pair instability SN of standard Pop III (less massive) stars are avoided so that one might avoid the constraint on their numbers. Other constraints on DS will arise from cosmological considerations. A first study of their effects (and those of the resultant MS stars) on reionization have been done by Schleicher et al. (2008a,2008b), and further work in this direction is warranted.

The resultant black holes from DS could be very important. DS would make plausible precursors of the $10^9 M_\odot$ black holes observed at $z = 6$ (Li et al. 2007; Pelopessy et al. 2007); of Intermediate Mass Black Holes; of black holes at the centers of galaxies; and of the black holes recently inferred as an explanation of the extragalactic radio excess seen by the ARCADE experiment (Seiffert et al. 2009). However, see Alvarez et al. (2008) who present caveats regarding the growth of early black holes. In addition, the black hole remnants from DS could play a role in high-redshift gamma ray bursts thought to take place due to accretion onto early black holes (we thank G. Kanbach for making us aware of this possibility).

In the presence of prolonged capture, the DS could end up even larger, possibly leading to supermassive stars that consume all the baryons in the original halo, i.e., possibly up to $10^5 M_\odot$ stars. The role of angular momentum during the accretion must be accounted for properly and will affect the final result; in fact, even for the $1000 M_\odot$ case studied in this paper, we intend to examine the possible effects of angular momentum. This possibility will be further investigated in a future publication (in preparation), both from the point of view of the stellar structure, as well as the consequences for the universe.

REFERENCES

Abel, T., Bryan, G. L., & Norman, M. L. 2002, Science, 295, 93

Alvarez, M. A., Wise, J. H., & Abel, T. 2008, arXiv:0811.0820 [astro-ph].

Bahcall, J. N. 1989, *Neutrino Astrophysics* (Cambridge: Cambridge Univ. Press)

Barkana, R, & Loeb, A. 2001, Phys. Rep., 349, 125

Barnes, J., & White, S. D. M. 1984, MNRAS, 211, 753

Bertone, G., Hooper, D., & Silk, J. 2005, Phys. Rep., 405, 279

Bertone, G., & Fairbairn, M. 2007, arXiv:0711.1485

Blumenthal, G. R., Faber, S. M., Flores, R., & Primack, J. R. 1986, ApJ, 301, 27

Bouquet, A., & Salati, P. 1989, ApJ, 346, 284

Bromm, V., & Larson, R. B. 2004, ARA&A, 42, 79

Chandrasekhar, S. 1939, An Introduction to the Study of Stellar Structure (Chicago: Univ. of Chicago Press)

Chang S., Pierce A., & Weiner N., arXiv:0808.0196 [hep-ph].

Clayton, D. D. 1968, *Principles of Stellar Evolution and Nucleosynthesis* (New York: McGraw-Hill)

Freese, K., Bodenheimer, P., Spolyar, D., & Gondolo, P. 2008a, Astrophys. J. **685**, L101 (2008), arXiv:0806.0617

Freese, K., Gondolo, P., Sellwood, J. A., & Spolyar, D. 2008b, arXiv:0805.3540

Freese, K., Spolyar, D., & Aguirre, A. 2008c, JCAP **11**, 014 (2008), arXiv:0802.1724

Gao, L., Abel, T., Frenk, C. S., Jenkins, A., Springel, V., & Yoshida, N. 2007, MNRAS, 378, 449

Gould, A. 1987a, ApJ, 321, 571

Griest, K.,& Seckel, D. 1987, Nuc. Phys. B, 283, 681

Heger, A., & Woosley, S. E. 2002, ApJ, 567, 532

Hollenbach, D., & McKee, C. F. 1979, ApJS, 41, 555

Hooper, D., & Profumo, S. 2007, Phys. Rept. 453, 29

Hooper, D., et al. 2009, Phys. Rev. D, 79, 015010 [arXiv:0808.2464 [hep-ph]].

Iglesias, C. A., & Rogers, F. J. 1996, ApJ, 464, 943

Iocco, F. 2008, ApJ, 667, L1

Iocco, F., Bressan, A., Ripamonti, E., Schneider, R., Ferrara, A., & Marigo, P. 2008, MNRAS, 390, 1655

Jungman, G., Kamionkowski, M., & Griest, K. 1996, Phys. Rept., 267, 195

Kippenhahn, R., & Weigert, A. 1990, Stellar Structure and Evolution (Berlin: Springer).

Krauss, L., Freese, K., Press, W., & Spergel, D. N. 1985, Ap J, 299, 1001

Lenzuni, P., Chernoff, D. F., & Salpeter, E. 1991, ApJS, 76, 759

Li, Y. X. et al 2007, ApJ, 665, 187

Matsuda, T., Sato, H., & Takeda, H. 1971, Prog. Theor. Phys., 46, 416

McKee, C. F., & Tan, J. C. 2008, ApJ, 681, 771

Moskalenko, I. V., & Wai, L. L. 2007, ApJ., 659, L29

Navarro, J. F., Frenk, C. S., & White, S. D. M. 1996, ApJ, 462, 563

Ohkubo, T. et al. 2006, ApJ, 645, 1352

Omukai, K., & Nishi, R. 1998, ApJ, 508, 141

O'Shea, B. W., & Norman, M. L. 2007, ApJ, 654, 66

Peebles, P. J. E., & Dicke, R. H. 1968, ApJ, 154, 891

Pelopessy, F. I., Di Matteo, T., & Ciardi, B. 2007, arXiv:astro-ph/0703773

Ripamonti, E., & Abel, T. 2005, arXiv:astro-ph/0507130.

Ripamonti, E., Mapelli, M., & Ferrara, A. 2007, MNRAS, 375, 1399

Ripamonti, & et. al. 2009, arXiv:0903.0346

Ryden, B. S., & Gunn, J. E. 1987, ApJ, 318, 15

Salati, P., & Silk, J. 1989, ApJ, 338, 24

Savage, C., Gondolo, P., & Freese, K. 2004, Phys. Rev. D, 70, 123513

Savage C., Gelmini G., Gondolo P., & Freese K., arXiv:0808.3607 [astro-ph].

Schaerer, D. 2002, A&A, 382, 28

Scott, P., Edsjo, J., & Fairbairn, M. 2007, arXiv:0711.0991

Scott, P., Fairbairn, M., & Edsjo, J. 2009, MNRAS, 394, 82

Schleicher, D. R. G., Banerjee, R., & Klessen, R. S. 2008a, Phys. Rev. D, **78**, 083005, [arXiv:0807.3802 [astro-ph]].

Schleicher, D. R. G., Banerjee, R., & Klessen, R. S. 2008b, arXiv:0809.1519 [astro-ph].

Seiffert, M. et al. 2009, arXiv:0901.0559 [astro-ph.CO].

Spolyar, D., Freese, K., & Gondolo, P. 2008, Phys. Rev. Lett., 100, 051101

Tan, J. C., & McKee, C. F. 2004, ApJ, 603, 383

Taoso, M., Bertone, G., Meynet, G., & Ekström, S. 2008, Phys. Rev. D., 78, 123510

Yoon, S.-C., Iocco, F., & Akiyama, S. 2008, ApJ, 688, L1

Yoshida, N., Abel, T., Hernquist, L., & Sugiyama, N. 2003, ApJ, 592, 645

Yoshida, N., Omukai, K., Hernquist, L., & Abel, T. 2006, ApJ, 652, 6

Young, P. 1980, ApJ, 242, 1232